BEC preprints 2025.1
doi 10.26124/becprep.2025-0001

Open Access

Experimental Communication

Cite
Donnelly C, Menoud V, Kayser B, Regazzi R, Jacovetti C (2025) Downregulation of the mitochondrial tRNA-derived fragment mt-tRF-Leu^{TAA} enhances skeletal muscle insulin sensitivity. BEC preprints 2025.1. https://doi.org/10.26124/becprep.2025-0001

Author contributions
CD performed the *in vitro* experiments using the differentiated C2C12 myotube cell line, analyzed and interpreted the results and wrote the manuscript and secured funding. VM performed experiments. BK provided insights into pathophysiological mechanisms and experiments to conduct, critically revised the manuscript and secured funding. RR contributed to the conception of the study, helped with interpretation of the data, critically revised and edited the manuscript and secured funding. CJ designed the study, conceived, performed, analyzed experiments, interpreted results and wrote the manuscript. All the authors approved the final version of the manuscript.

Funding
This work was supported by the Swiss National Science Foundation (#310030_188447 and #310030_219252 to R.R. and #194964 to C.D.).

Conflicts of interest
No conflicts of interest to declare.

Received 2025-04-17
Accepted 2025-04-17
Online 2025-04-17

Data availability
Data are available upon request to the corresponding author.

Downregulation of the mitochondrial tRNA-derived fragment mt-tRF-Leu^{TAA} enhances skeletal muscle insulin sensitivity

Donnelly C[1], Menoud V[2], Kayser B[1], Regazzi R[2,3,4], Jacovetti C[2,4]

[1] Institute of Sport Sciences, University of Lausanne, CH
[2] Department of Fundamental Neurosciences, University of Lausanne, CH
[3] Department of Biomedical Sciences, University of Lausanne, CH
[4] These authors contributed equally

Corresponding author: cecile.jacovetti@unil.ch

Summary

The mitochondrial tRNA-derived fragment mt-tRF-Leu^{TAA} couples mitochondrial metabolism to insulin secretion. While its role in pancreatic β-cell function is well established, its broader impact on multi-organ glucose homeostasis remains unclear. In insulin target tissues, the presence, regulation, and mechanism of action of mt-tRF-Leu^{TAA} are entirely unexplored. This study addresses this gap by investigating the impact of diet, nutritional status and diabetes on mt-tRF-Leu^{TAA} regulation and by assessing its role in insulin sensitivity. We examined mt-tRF-Leu^{TAA} levels in different insulin target tissues, including skeletal muscle, liver, and epididymal white adipose tissue, of rodents under physiological and pathological conditions. In skeletal muscle myotubes, we combined subcellular fractionation, antisense oligonucleotide-mediated knockdown and glucose uptake assays to determine mt-tRF-Leu^{TAA}'s mitochondrial localization and its influence on insulin sensitivity. mt-tRF-Leu^{TAA} levels in mouse skeletal muscle decreased twofold in response to fasting. In myotubes, this tRNA fragment was enriched in mitochondria, and its downregulation enhanced glucose uptake. While the levels of mt-tRF-Leu^{TAA} remained unchanged in insulin target tissues of diabetic mice, we observed a skeletal muscle-specific downregulation of mt-tRF-Leu^{TAA} in young adult rats

Keywords – Mitochondrially-encoded tRNAs / mt-tRNA-derived fragments / Nutritional status / Muscle glucose uptake / Diabetes susceptibility

exhibiting insulin hypersensitivity. This study identifies mt-tRF-Leu^{TAA} as a regulator of skeletal muscle insulin sensitivity. By modulating both insulin secretion and action, mt-tRF-Leu^{TAA} emerges as a critical player in systemic metabolic control, offering a promising target for diabetes treatment.

1. Introduction

In response to rising postprandial glycaemia, pancreatic β-cells sense, uptake and metabolize carbohydrates, with mitochondrial ATP generation triggering insulin release (Nicholls, 2016). We recently identified a mitochondrial tRNA-derived fragment, mt-tRF-Leu^{TAA}, as a key regulator linking mitochondrial metabolism to insulin secretion (Jacovetti *et al.,* 2024). Mechanistically, mt-tRF-Leu^{TAA} interacts with core subunits and assembly factors of respiratory complexes in the mitochondrial electron transfer system, modulating ATP production and insulin secretion in β-cells (Jacovetti *et al.,* 2024). However, despite this established role in β-cell function, the broader impact of mt-tRF-Leu^{TAA} on multi-organ glucose homeostasis remains unclear.

Glucose regulation relies on a coordinated network of organs beyond the pancreas (Petersen and Shulman 2018; Röder *et al.,* 2016). Once secreted, insulin binds to receptors in muscle, liver, and adipose tissues, promoting glucose uptake, inhibiting hepatic glucose production, and driving glycogenesis, lipogenesis, and protein synthesis, ultimately lowering blood glucose levels (Petersen and Shulman 2018; Röder *et al.,* 2016). Notably, liver and muscle account for 70% of postprandial glucose clearance (Moore et al., 2012; DeFronzo and Tripathy, 2009). This intricate interplay between glucose sensing, insulin secretion and glucose disposal is essential for metabolic homeostasis and its disruption contributes to diabetes development (Petersen and Shulman 2018; Röder *et al.,* 2016).

Despite the well-established role of reduced insulin sensitivity in diabetes onset, the function of mitochondrial tRNA-derived fragments in this context remains poorly understood (Jacovetti et al., 2021; Arroyo *et al.,* 2021). Given the conserved genome of mitochondria across tissues (Herbers *et al.,* 2019), mt-tRF-Leu^{TAA} is likely to be present also in mitochondria of insulin target tissues. Since mt-tRF-Leu^{TAA} regulates mitochondrial electron transfer and ATP generation, two critical processes for insulin responsiveness (Kim *et al.,* 2008, Henver *et al.,* 2022), it emerges as a potential metabolic regulator not only in β-cells but also in insulin-responsive tissues.

Here, we examined mt-tRF-Leu^{TAA} levels in insulin target tissues, including muscle, liver, and epididymal white adipose tissue under physiological and pathological conditions. We observed a downregulation of mt-tRF-Leu^{TAA} in skeletal muscle during fasting and in a model of diabetes susceptibility. While mt-tRF-Leu^{TAA} depletion impairs glucose stimulated insulin secretion in pancreatic β-cells (Jacovetti *et al.,* 2024), we now reveal that its inhibition enhances insulin sensitivity in skeletal muscle. These findings highlight mt-tRF-Leu^{TAA} as a pivotal regulator of systemic metabolic control, influencing both insulin secretion and action.

2. Results

2.1 mt-tRF-LeuTAA levels in insulin target tissues under physiological conditions

To investigate the involvement of the mitochondrial fragment mt-tRF-Leu^{TAA} in peripheral insulin target tissues under physiological conditions, we employed the same study design that previously revealed its dynamic response to fasting-refeeding cycles in pancreatic islets (Jacovetti *et al.,* 2024). C57BL/6 mice underwent a 2-hour fasting period, followed by a single oral dose of 2 mg per g of body weight glucose solution to reset digestive functions and glycogen stores. Some mice were sacrificed after 30 minutes (Fed group), while others underwent a 16-hour fasting period before receiving a single oral dose of water (Fasted group) or glucose (Post-prandial group; Figure 1A). Blood glucose levels were monitored to ensure proper carbohydrate administration (Jacovetti *et al.,* 2024) and the g*astrocnemius* muscle, the liver and epididymal white adipose tissue were collected for analysis (Figure 1A).

qRT-PCR analysis revealed that mt-tRF-Leu^{TAA} levels in the *gastrocnemius* muscle decrease nearly twofold in response to fasting (Figure 1B). These levels did not recover following refeeding and remained reduced at two hours post-prandial (Figure 1B). Importantly, these fluctuations in mt-tRF-Leu^{TAA} levels occurred independently of changes in its parental tRNA, mt-tRNA-Leu^{TAA}, across all conditions (Figure 1C). As previously observed in pancreatic islets, these changes appear rapid, dynamic, independent of the host tRNA and specific to mt-tRF-Leu^{TAA}. Indeed, other mitochondrial- and nuclear-encoded fragments, mt-tRF-Gln^{TTG} and nc-tRF-Asp^{GTC}, remained unaltered in skeletal muscle during fasting and refeeding (Figure 1D, E).

In contrast, mt-tRF-Leu^{TAA} levels in the liver remained stable during fasting but increased significantly post-prandially (Figure 1F). Similar to skeletal muscle, mt-tRNA-Leu^{TAA}, mt-tRF-Gln^{TTG} and nc-tRF-Asp^{GTC} were unchanged in all conditions (Figure 1G-I). In epididymal white adipose tissue, none of these fragments exhibited significant alterations in response to fasting or refeeding (Figure 1J-M).

Calculating the ratio of the host tRNA to mt-tRF-Leu^{TAA} using the data presented above (Figures 1B, C, F, G, J, K) and those previously published for pancreatic islets (Jacovetti *et al.,* 2024), confirmed the dynamic response of mt-tRF-Leu^{TAA} to fasting and refeeding in the pancreatic islets and corroborated its fasting-induced decrease in skeletal muscle (Figure 1N). The magnitude of this twofold reduction closely mirrored that observed in the pancreatic islets (Figure 1N). Given our previous findings demonstrating that modulating mt-tRF-Leu^{TAA} levels in β-cells affects glucose-stimulated insulin secretion (Jacovetti *et al.,* 2024), it is plausible that fasting-induced reductions of mt-tRF-Leu^{TAA} in skeletal muscle may influence insulin sensitivity (Kido *et al.,* 2022; Jørgensen *et al.,* 2021). This possibility led us to further explore the functional consequences of mt-tRF-Leu^{TAA} downregulation on skeletal muscle insulin sensitivity.

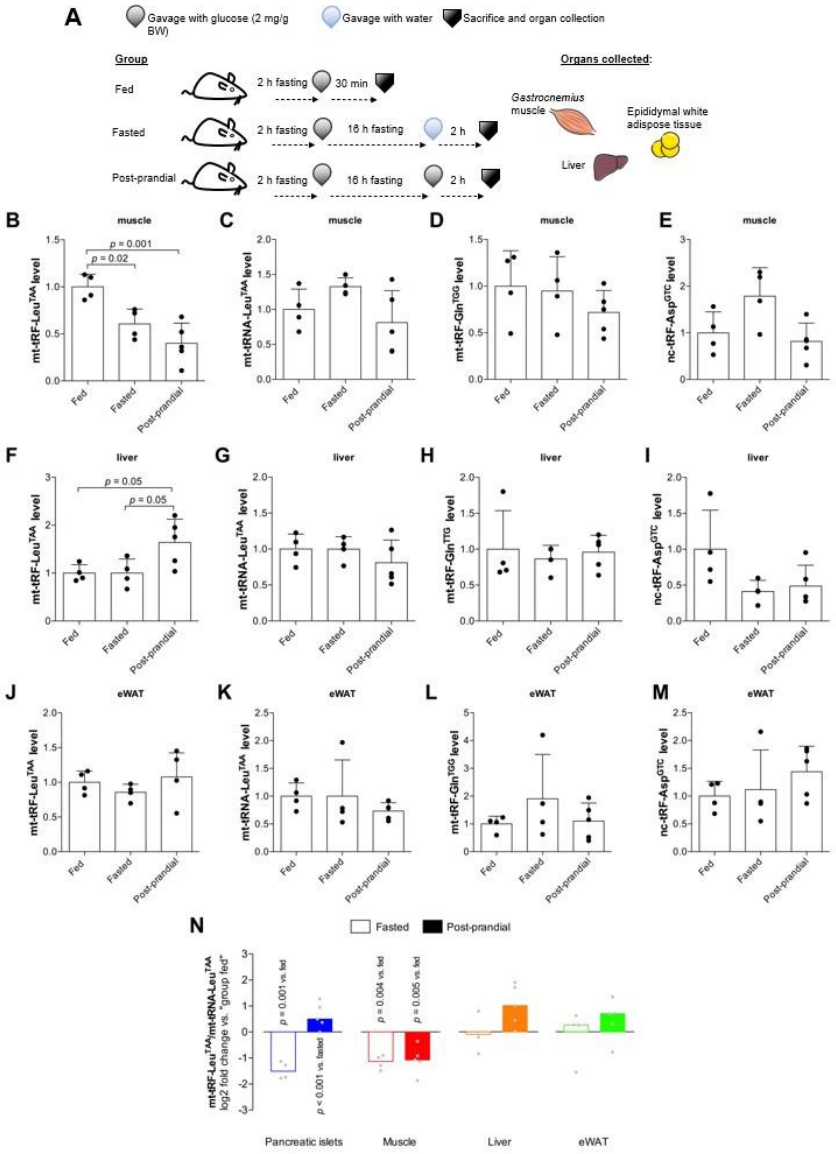

Figure 1. Changes in mt-tRF-LeuTAA levels during fasting and refeeding in insulin target tissues. A) Schematic representation of the experiment, including timing of interventions and nutritional supplies for each group. The gastrocnemius muscle, liver and epididymal white adipose tissue were collected after sacrifice of the mice. B-M) Changes of tRNA-fragments in response to fasting and refeeding in different insulin target tissues. The data are presented as fold changes over the fed condition. Levels in gastrocnemius muscle of (B) mt-tRF-LeuTAA, (C) the parental tRNA mt-tRNA-LeuTAA, (D) the mitochondrially-encoded fragment mt-tRF-GlnTTG and (E) the nuclear-encoded fragment nc-tRF-AspGTC. Levels in the liver of (F) mt-tRF-LeuTAA, (G) mt-tRNA-LeuTAA, (H) mt-tRF-GlnTTG and (I) nc-tRF-AspGTC. Levels in epididymal white adipose tissue (eWAT) of (J) mt-tRF-LeuTAA, (K) mt-tRNA-LeuTAA, (L) mt-tRF-GlnTTG and (M) nc-tRF-AspGTC. (N) Changes in mt-tRF-LeuTAA/mt-tRNA-LeuTAA ratio in response to fasting and refeeding in pancreatic islets (Jacovetti et al., 2024), gastrocnemius muscle, liver and epididymal white adipose tissue. The bars represent the means, error bars the standard deviations and dots individual values. N = 4-5, one-way ANOVA with Dunnett post-hoc test.

2.2 Silencing mt-tRF-LeuTAA in skeletal muscle enhances insulin sensitivity

To assess whether fasting-induced reduction of mt-tRF-Leu^{TAA} in skeletal muscle influences insulin sensitivity, we used well-differentiated C2C12 myotube cells, a model known to take up and metabolize glucose in response to insulin stimulation (Abdelmoez *et al.,* 2020) and contraction (Abdelmoez *et al.,* 2020; Donnelly *et al.,* 2024).

First, we confirmed the presence of the mt-tRF-Leu^{TAA} in mitochondrial fractions of myotubes (Figure 2A; for culture protocol see Donnelly *et al.,* 2024). Our previous study showed that mt-tRF-Leu^{TAA} is approximately ten times more abundant in mitochondria-enriched fractions compared to whole cell lysates in human and rodent islet cells (Jacovetti *et al.,* 2024) and similar enrichments were observed in differentiated C2C12 myotubes (Figure 2A).

To functionally assess the impact of mt-tRF-Leu^{TAA} downregulation, we transfected myotube cells with antisense oligonucleotides (Figure 2B). As previously demonstrated, antisense anti-tRF-Leu^{TAA} specifically binds to mt-tRF-Leu^{TAA} but not to the parental tRNA (Jacovetti *et al.,* 2024). We confirmed that successful delivery of the antisense oligonucleotide resulted in over 80% suppression of mt-tRF-Leu^{TAA} in mitochondrial fractions of myotube cells (Figure 2B). This inhibition significantly enhanced insulin-mediated glucose uptake in muscle cells (Figure 2C).

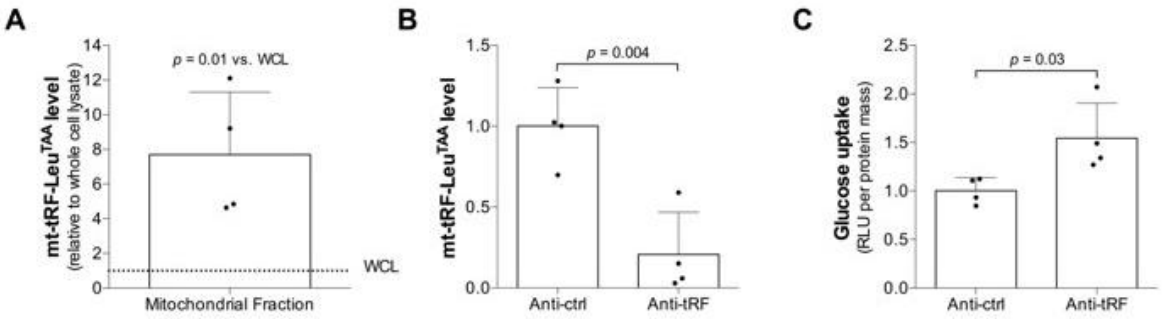

Figure 2. Silencing the mt-tRF-LeuTAA in skeletal muscle enhances insulin sensitivity. A) Fold enrichment relative to whole cell lysate of mt-tRF-LeuTAA in mitochondrial preparations of mouse C2C12 myotubes. Data are expressed as fold change relative to whole cell lysate ± SD of 4 independent experiments, one-sample Student's t-test. B) Inhibition of mt-tRF-LeuTAA in mitochondrial preparations of C2C12 myotubes upon transfection of control (anti-ctrl) or antisense mt-tRF-LeuTAA (anti-tRF) oligonucleotides. The level of mt-tRF-LeuTAA was determined by qRT-PCR. Data are presented as fold change relative to control ± SD, N = 4, unpaired Student's t-test. C) Insulin-induced glucose uptake in C2C12 myotubes upon inhibition of mt-tRF-LeuTAA. Relative light units RLU. Results are expressed as fold changes ± SD of 4 separate sets of cells transfected with control (anti-ctrl) vs anti-mt-tRF-LeuTAA (anti-tRF) oligonucleotides, N = 4 unpaired Student's t-tests.

Overall, these findings indicate that mt-tRF-Leu^{TAA} downregulation enhances skeletal muscle insulin sensitivity. Thus, given its established role in modulating glucose metabolism and insulin secretion, mt-tRF-Leu^{TAA} may represent a key regulator of metabolic homeostasis.

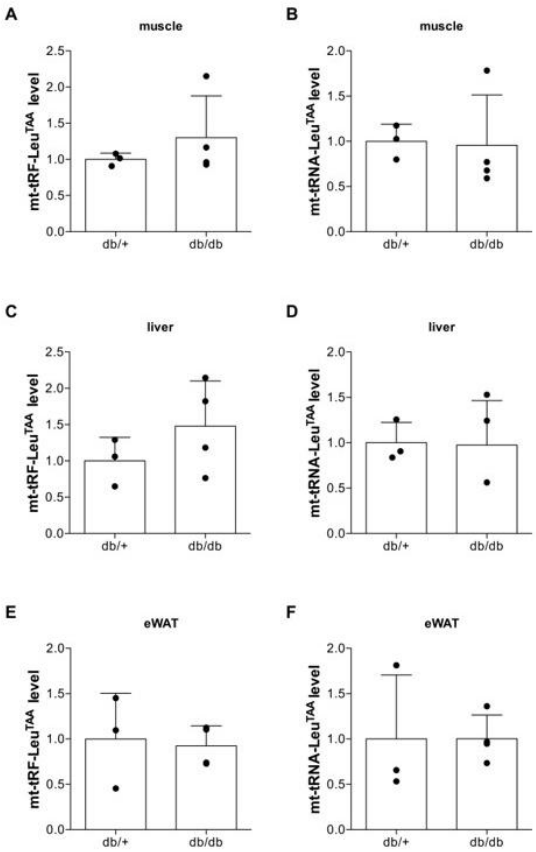

Figure 3. mt-tRF-LeuTAA levels in insulin target tissues of diabetic mice. mt-tRF-LeuTAA (A) and mt-tRNA-LeuTAA (B) levels in the gastrocnemius muscle of control heterozygote db/+ and db/db mice. mt-tRF-LeuTAA (C) and mt-tRNA-LeuTAA (D) levels in the liver of control heterozygote db/+ and db/db mice. mt-tRF-LeuTAA (E) and mt-tRNA-LeuTAA (F) levels in epididymal white adipose tissue (eWAT) of control heterozygote db/+ and db/db mice. The data are expressed as fold changes over the level in db/+ mice. Bars represent the means, error bars the standard deviations and the dots the individual values. N = 3-4, unpaired Student's t-tests.

2.3 In diabetic mice mt-tRF-LeuTAA is downregulated in the pancreatic islets but not insulin target tissues

Since diabetes is characterized by impaired insulin secretion and sensitivity, as well as a downregulation of mt-tRF-Leu^{TAA} levels in pancreatic islets (Jacovetti *et al.,* 2024), we investigated whether mt-tRF-Leu^{TAA} levels are altered also in insulin target tissues of diabetic animals. For this purpose, we examined the levels of mt-tRF-Leu^{TAA} in the g*astrocnemius* muscle, liver and epididymal white adipose tissue of diabetic *db/db* mice, which carry a mutation in the leptin receptor and are hyperphagic, obese and exhibit fasting hyperglycaemia (Jacovetti *et al.,* 2024, Peyot *et al.,* 2010; Suriano *et al.,* 2021). qRT-PCR analysis revealed no significant changes in mt-tRF-Leu^{TAA} or its parental tRNA mt-tRNA-Leu^{TAA} (Figure 3A-F). Thus, unlike the fasting-refeeding cycle, diabetes-induced downregulation of mt-tRF-Leu^{TAA} is restricted to pancreatic islets (Jacovetti *et al.,* 2024).

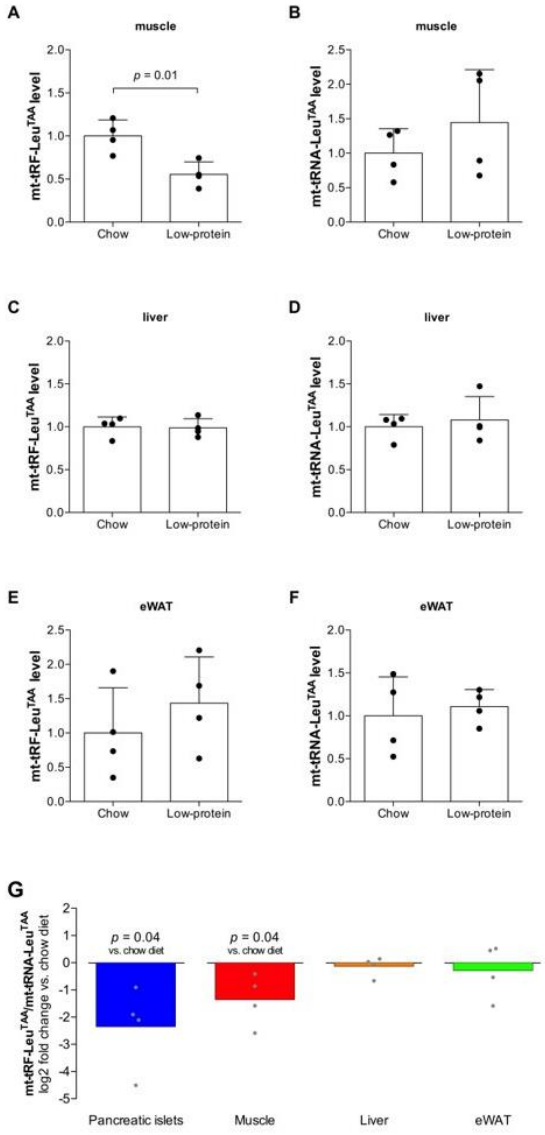

Figure 4. mt-tRF-LeuTAA levels in insulin target tissues of young rats exhibiting insulin hypersensitivity and impaired insulin secretion. mt-tRF-LeuTAA (A) and mt-tRNA-LeuTAA (B) levels in the gastrocnemius muscle of the offspring of rats fed a low-protein diet (Low-protein) or an isocaloric control diet (Chow). mt-tRF-LeuTAA (C) and mt-tRNA-LeuTAA (D) levels in the liver of chow diet and low-protein exposed rats. mt-tRF-LeuTAA (E) and mt-tRNA-LeuTAA (F) levels in the epididymal white adipose tissue (eWAT) of chow diet and low-protein exposed rats. (G) Changes in the mt-tRF-LeuTAA/mt-tRNA-LeuTAA ratio in pancreatic islets (Jacovetti et al., 2024), gastrocnemius muscle, liver and epididymal white adipose tissue in response to low-protein exposure during gestation and lactation. The data are expressed as fold changes over the level in Chow. The bars represent the means, error bars the standard deviations, dots are individual values. N = 4, unpaired Student's t-tests.

2.4 Muscle-specific downregulation of mt-tRF-LeuTAA in young adult rats exhibiting insulin hypersensitivity

To determine whether mt-tRF-Leu^{TAA} alterations occur in insulin target tissues in pre-diabetic conditions, we examined the levels of the mitochondrial fragment in a model of diabetes-prone rats. This model comprises 22-day-old rats born to mothers fed a low-protein (LP) diet during pregnancy and lactation (Jacovetti *et al.,* 2024). These animals exhibit impaired postnatal pancreatic β-cell mass expansion, mitochondrial dysfunction, defective glucose-stimulated insulin secretion, and initially heightened insulin sensitivity, which later progresses to insulin resistance and glucose intolerance in adulthood (Martins *et al.,* 2018; Thorn *et al.,* 2011).

qRT-PCR analysis revealed that mt-tRF-Leu^{TAA} levels are significantly reduced in the *gastrocnemius* muscle of LP-exposed 22-day-old rats compared to controls (Figure 4A) while the host tRNA, mt-tRNA-Leu^{TAA}, remained unchanged (Figure 4B). No significant alterations were observed in the liver and epididymal white adipose tissue (Figure 4C-F). The mt-tRF-Leu^{TAA}/mt-tRNA-Leu^{TAA} ratio further confirmed a significant downregulation of mt-tRF-Leu^{TAA} in both pancreatic islets and skeletal muscle (Figure 4G), in these insulin hypersensitive young rats.

Overall, our findings demonstrate that downregulation of the mitochondrial tRNA-derived fragment mt-tRF-Leu^{TAA} enhances skeletal muscle insulin sensitivity and suggest a pivotal role in systemic metabolic control by regulating both insulin secretion (Jacovetti *et al.,* 2024) and insulin action.

3. Discussion

The mitochondrial tRNA-derived fragment mt-tRF-Leu^{TAA}, couples mitochondrial metabolism to insulin secretion (Jacovetti *et al.,* 2024). However, its role in insulin target tissues and in diabetes susceptibility remains unexplored. Given the conservation of the mitochondrial genome across tissues and the central role of mitochondria in peripheral insulin sensitivity, we investigated mt-tRF-Leu^{TAA} levels in insulin-responsive tissues (muscle, liver, and epididymal white adipose tissue) under pathophysiological conditions. We observed a downregulation of mt-tRF-Leu^{TAA} in skeletal muscle in response to fasting and in a model of diabetes susceptibility. Notably, inhibiting mt-tRF-Leu^{TAA} enhanced insulin sensitivity in skeletal muscle. These findings suggest that mt-tRF-Leu^{TAA} plays a critical role in systemic metabolic control by modulating insulin secretion and responsiveness, offering a novel therapeutic target for mitochondrial diseases and diabetes prevention.

Glucose homeostasis relies on a finely tuned balance between insulin sensitivity in peripheral tissues (muscle, liver, and fat) and insulin secretion (Petersen and Shulman 2018; Röder *et al.,* 2016). Skeletal muscle, as the primary site of postprandial glucose uptake, and pancreatic β-cells, which adapt insulin secretion to maintain glucose levels, are key players in glucose regulation (DeFronzo and Tripathy, 2009; Petersen and Shulman 2018). Early defects in glucose-stimulated insulin secretion and skeletal muscle insulin resistance are pivotal in diabetes progression (DeFronzo and Tripathy, 2009; Petersen and Shulman 2018; Röder *et al.,* 2016). The dynamic regulation of mt-tRF-Leu^{TAA} in skeletal muscle aligns with mitochondria's essential role in insulin sensitivity. Prolonged fasting or a low-protein diet, which mimic nutrient scarcity, are associated with reduced mt-tRF-Leu^{TAA} levels and enhanced insulin sensitivity (Martins *et al.,* 2018; Thorn *et al.,* 2011; Vipin *et al.,* 2022; Heijboer *et al.,* 2005; Fontana *et al.,* 2010). Muscle

insulin sensitivity increases after starvation, promoting glucose uptake to sustain muscle function under limited nutrient availability (Heijboer *et al.,* 2005). Furthermore, different studies reported a "metabolic memory" post-starvation, whereby insulin sensitivity remains elevated for a short period after refeeding, possibly to preemptively adapt to potential future nutrient scarcity (Heijboer *et al.,* 2005). In agreement with this observation, mt-tRF-Leu^{TAA} levels remained low 2-hour post refeeding. *In vitro* silencing of this mitochondrial fragment in myotube cells reproduces the enhanced glucose uptake associated with these physiological conditions (Figure 2C). The molecular mechanisms underlying this process remain to be explored, but open exciting new avenues for future research on how mt-tRF-Leu^{TAA} contributes to insulin signaling pathways.

Blocking mt-tRF-Leu^{TAA} in β-cells reduces OXPHOS capacity and disrupts mitochondrial ATP regeneration (Jacovetti *et al.,* 2024). While impaired mitochondrial coupling is unequivocally linked to defective GSIS (Sivitz et Yorek, 2010), its impact in insulin target tissues is more complex. Depending on the tissue, mitochondrial respiration defects can either induce insulin resistance or enhance insulin sensitivity (Sivitz et Yorek, 2010, Holloszy, 2013; Timper *et al.,* 2018). Notably, in some pathological conditions characterized by defective mitochondrial oxidative phosphorylation, insulin action is paradoxically improved (Holloszy, 2013). The observed downregulation of mt-tRF-Leu^{TAA} in muscle after prolonged fasting and in diabetes-prone rats may contribute to this remarkable adaptive mechanism. Skeletal muscle insulin sensitivity is enhanced by physical activity, another physiological state associated with acutely reduced OXPHOS capacities resulting from the contractile demands of exercise (Holloszy, 2011; Trewin *et al.,* 2018; Parker et al., 2018). Exploring the regulation of the mitochondrial fragment under this condition would be particularly insightful.

Interestingly, mt-tRF-Leu^{TAA} levels remain unchanged in the muscle of obese diabetic *db/db* mice, which exhibit insulin resistance and glucose intolerance (Peyot *et al.,* 2010; Suriano *et al.,* 2021). The lack of mt-tRF-Leu^{TAA} reduction in muscle may be directly tied to muscle insulin resistance in these mice.

Contrary to skeletal muscle, mt-tRF-Leu^{TAA} levels in the liver increase and exceed basal levels following refeeding after prolonged fasting. This may reflect hepatic adaptation in glucose production, glycogen mobilization and lipid storage (Heijober *et al.,* 2005; Titchenell *et al.,* 2017).

The ongoing debate in diabetes research questions whether insulin resistance or insulin hypersecretion is the primary cause of type 2 diabetes (Nolan and Prentki, 2019). Initially considered a beneficial compensatory response, chronic insulin hypersecretion is now considered as detrimental, contributing to β-cell exhaustion, promoting hepatic gluconeogenesis and lipogenesis, and systemic insulin resistance (Nolan and Prentki, 2019). Thus, reducing mt-tRF-Leu^{TAA} levels may provide dual benefits: mitigating excessive glucose stimulated insulin secretion while enhancing muscle insulin sensitivity.

We previously found that pharmacological inhibition of mTORC1 in β-cells reduces mt-tRF-Leu^{TAA} levels (Jacovetti *et al.,* 2024). Consistent with the effects of mTORC1 inhibitors (Blagosklonny, 2019), downregulation of mt-tRF-Leu^{TAA} leads to a decrease in insulin secretion and enhanced insulin sensitivity in myotubes. Given that mTORC1 synchronizes metabolic responses across multiple tissues (Gonzalez, 2017), it is plausible that its effects are partially mediated via mt-tRF-Leu^{TAA} regulation. Metformin and rapamycin, both mTORC1 inhibitors, improve metabolic health in diabetes (Laplante and Sabatini, 2012), highlighting the potential of targeting mt-tRF-Leu^{TAA} for therapeutic intervention.

4. Conclusion

In summary, our study demonstrates that downregulation of the mitochondrial tRNA-derived fragment mt-tRF-Leu^{TAA} enhances skeletal muscle insulin sensitivity. By modulating both insulin secretion and action, mt-tRF-Leu^{TAA} emerges as a critical player in systemic metabolic control, offering a promising target for mitochondrial disease and diabetes treatment.

5.Materials and methods

Table 1. Key resource table

REAGENT OR RESOURCE	SOURCE	IDENTIFIER
CHEMICALS, PEPTIDES AND ENZYMES		
Bradford assay	Thermo Fischer Scientific	Cat#23246
D-(+)-glucose solution	Sigma-Merck	Cat#G8769-100ml
DNase	Promega	Cat#M6101
DMEM	Thermo Fisher Scientific	Cat#41966
Fetal bovine serum	Thermo Fisher Scientific	Cat#1008247
Glucose Uptake-Glo™ Assay kit	Promega	Cat#J1341
Insulin	Merck-Sigma	#I9278
Lipofectamine 2000	Thermo Fischer Scientific	#11668019
miRCURY LNA Universal RT microRNA PCR system	Qiagen	#339340 for RT kit and #339347 for Sybr Green
M-MLV reverse transcriptase	Promega	#M3683
miRNeasy micro kit	Qiagen	#217084
miRNeasy mini kit	Qiagen	#217004
Non-essential amino acids	Thermo Fisher Scientific	#11140035
Penicillin streptomycin	Thermo Fisher Scientific	#15140122
QIAquick gel extraction kit	Qiagen	#28704
QIAzol lysis reagent	Qiagen	#79306
Random primers	Promega	#C1181
SsoAdvanced Universal SYBR Green Supermix	BioRad	#1725274
EXPERIMENTAL MODELS: STRAINS		
BKS(D)-Leprdb/+/JorlRj (db/+) (M. musculus)	Janvier Laboratories	n/a
BKS(D)-Leprdb/JorlRj (db/db) (M. musculus)	Janvier Laboratories	n/a
Sprague Dawley (R. norvegicus)	Janvier Laboratories	n/a
C57BL/6J (M. musculus)	Janvier Laboratories	n/a
SPECIAL DIETS		
Low protein diet	Safe diet	U8959P Version 0156
Isocaloric control diet	Safe diet	U8978P Version 0022

EXPERIMENTAL MODELS: CELL LINES		
C2C12 cells	ATCC	Cat#Crl-1772

5.1 Experimental models

Animals were grouped (3-4 mice or 4 rats per cage), except for pregnant females, which were housed alone. They were kept under a 12-hour light/dark cycle, with controlled temperature (20-24°C) and humidity (40-70%). Apart from fasting/refeeding cycles and special diets, animals had ad libitum access to water and standard chow. All procedures followed the National Institutes of Health guidelines and were approved by the national health and medical research council of Australia and the Swiss research council and veterinary offices (authorization VD2495, VD2824 and VD2824; Jacovetti *et al.,* 2024). C57BL/6 female mice and pregnant Sprague Dawley rats were obtained from Janvier Laboratories (Le Genest-Saint-Isle, France).

For fasting/refeeding cycle experiments, 12-weeks-old C57BL/6J female mice were used. Mice were subjected to a 2-hour period without food, followed by a single oral dose of 2 mg/g body weight glucose solution to reset digestive functions and glycogen stores. From these mice, some were sacrificed after 30 minutes (fed group) and the others underwent a 16-hour fasting and were sacrificed 2 hours after a single oral dose of water (fasted group) or glucose (post-prandial group; Figure 1A). Blood glucose levels were monitored to ensure proper carbohydrate administration and the g*astrocnemius* muscle, the liver and epididymal white adipose tissue were collected (Figure 1A). For each mouse, gavage success was checked by measuring blood glucose 30 minutes after the *per os* administration. A blood drop was collected from a tail snip by gentle massaging and analyzed using a glucometer.

A first batch of 16-weeks-old *db/db* mice and their heterozygote controls (*db/+*), was sourced from the Garvan Institute breeding colonies (Jacovetti *et al.,* 2012, Nesca *et al.,* 2013). A second batch of 11-weeks-old *db/db* mice (BKS(D)-Leprdb/JOrlRj) and their controls (BKS(D)-Leprdb/+/JorlRj) was obtained from Janvier Laboratories (Le Genest).

Pregnant Sprague Dawley rats were fed either a low-protein diet (5.3% protein, 17% fat, 77.7% carbohydrate) or an isocaloric control diet (16.8% protein, 17.4% fat, 65.8% carbohydrate) from day 2 of pregnancy through lactation, with progeny weaned and sacrificed 22 days after birth.

5.2 Tissue collection from animals

After C57BL/6 mice were sacrificed by cervical dislocation, the g*astrocnemius* muscle, the liver and epididymal white adipose tissue were dissected, washed with PBS and immediately snap-frozen in liquid nitrogen. Samples were disrupted and homogenized in 700 µL QIAzol lysis reagent and stored at -80 °C until RNA extraction.

5.3 C2C12 cell culture

C2C12 mouse skeletal muscle myoblasts (American Type Culture Collection) were cultured in proliferation medium composed of Dulbecco's modified Eagle's medium (DMEM) supplemented with 10 % fetal bovine serum, 100 IU/mL penicillin, 100 µg/mL streptomycin and maintained at 37 °C in a humidified atmosphere with 5 % O_2 and 5 % CO_2 (Binder Incubators). Once myoblasts reached 80-90 % confluence, the cells were differentiated by replacing the proliferation medium with a differentiation medium

consisting of DMEM supplemented with 2 % horse serum, 100 IU/mL penicillin, 100 µg/mL streptomycin and 1 % non-essential amino acids.

5.4 Isolation of mitochondrial fraction

Mitochondria were isolated from mouse C2C12 myotube cells as previously set up and validated (Lampl et al., 2015). The separation of mitochondrial and cytosolic fractions was performed on ice throughout the whole procedure as previously described in Jacovetti *et al.,* 2024.

5.5 RNA extraction

After rodent skeletal muscle, liver and epididymyal adipose tissue and C2C12 myotubes were resuspended in 700 µL QIAzol lysis reagent, and vortexed for 30 seconds, total RNA was extracted using miRNeasy mini or micro kit and treated with DNAse.

5.6 Total RNA and qPCR

Total RNA from rodent skeletal muscle, liver, epididymal adipose tissue, and C2C12 myotubes was reverse transcribed with M-MLV reverse transcriptase and random primers using 500ng of RNA. Quantitative PCR (qPCR) was performed with SsoAdvanced Universal SYBR Green Supermix. For host tRNA amplification, qPCR products were loaded on agarose gels, purified with the QIAquick gel extraction kit and confirmed to produce a single band (~75-80 bp). Primer efficiency was evaluated using standard curves. RNA levels were analyzed using the 2–ΔΔCt method, comparing host tRNA gene expression between samples. Normalization was done by calculating the ratio of 2–ΔΔCt values for the gene of interest against the reference gene, Hypoxanthine Phosphoribosyltransferase (Hprt). Primer sequences are listed in Jacovetti *et al.,* 2024.

5.7 tRF quantification by real-time PCR

Real-time PCR quantification of tRNA-derived fragments was performed using the miRCURY LNA Universal RT microRNA PCR system with 160 ng of RNA. Relative RNA levels between samples were calculated using the delta-delta Ct method (2–ΔΔCt). tRF abundance was normalized by dividing it by the mean relative expression of two microRNAs, miR-7 and let-7a-5p, which served as housekeeping small non-coding RNAs, unaffected by the study conditions. The input sequences used for primer design are indicated in Jacovetti *et al.,* 2024.

5.8 Cell transfection to inhibit mt-tRF-LeuTAA

Differentiated C2C12 myotubes were transfected with 30 picomoles single-stranded antisense oligonucleotides that correspond to the complementary sequence of the targeted tRF (Qiagen #custom power inhibitor PS desalted) or scrambled control oligonucleotides using Lipofectamine 2000. The sequence of antisense oligos anti-mmu-mt-tRF-Leu^{TAA} was: TGGGAACAAGGTTTTAAGTCT. Cells were then cultured for 48h before RNA extraction or glucose uptake assay.

5.9 Glucose uptake assay

On the day before the assay, the differentiation media was replaced with DMEM containing no serum. At the time of the assay, the culture medium was removed, and cells were washed with PBS pre-heated to 37 °C. They were then incubated with DMEM containing 1 µM insulin for 1 h. At the end of the incubation, the solution was removed, and the cells were incubated with 0.1 mM 2-deoxyglucose for 30 min. The uptake process was stopped and luciferase activities were measured using a Glucose Uptake-Glo Assay kit and a plate reader (BioTek). Cellular protein contents were determined by sampling a portion of the well content for quantitation via Bradford assay. Glucose uptake was analyzed according to the manufacturer's instructions (Donnelly *et al.*, 2024).

5.10 Quantification and statistical analysis

Data analysis as well as graphs and plots were performed in Excel and GraphPad Prism version 8.0.0 for Windows (GraphPad Software, San Diego, California USA, www.graphpad.com). Fold changes relative to control were calculated as [fold change = (value – control)/control]. The conditions used as control were: the fed group for fasting/refeeding experiments, db/+ for diabetic mice experiments and chow diet for the diabetes susceptibility experiments. The ratio mt-tRF-Leu^{TAA}/mt-tRNA-Leu^{TAA} level was calculated as [mt-tRF-Leu^{TAA}/mt-tRNA-Leu^{TAA} level = mt-tRF-Leu^{TAA} level/mt-tRNA-Leu^{TAA} level]. The data for the calculation of the ratios in pancreatic islets were taken from Jacovetti *et al.,* 2024.

To compare a data set to a control value set to 1, one-sample Student's *t*-test was used. For pairwise comparisons, statistical differences were assessed by two-tailed unpaired Student's *t*-test. In the case of multiple comparisons involving a single variable a one-way ANOVA followed by a Tukey post-hoc test was used. Statistical significance was considered whenever *p*-values were ≤ 0.05.

Acknowledgements

We warmly thank Dr. Ross Laybutt for providing RNA from *db/db* and *db/+* mice (Jacovetti *et al.,* 2012, Nesca *et al.,* 2013) and Jérémy Vidal for technical assistance. The graphical illustrations were made using Servier Medical Art (https://www.servier.com).

References

Abdelmoez AM, Sardón Puig L, Smith JAB, Gabriel BM, Savikj M, Dollet L, Chibalin AV, Krook A, Zierath JR, Pillon NJ (2020) Comparative profiling of skeletal muscle models reveals heterogeneity of transcriptome and metabolism https://doi.org/10.1152/ajpcell.00540.2019

Arroyo MN, Green JA, Cnop M, Igoillo-Esteve M (2021) tRNA Biology in the Pathogenesis of Diabetes: Role of Genetic and Environmental Factors https://doi.org/10.3390/ijms22020496

Blagosklonny MV (2019) Fasting and rapamycin: diabetes versus benevolent glucose intolerance https://doi.org/10.1038/s41419-019-1822-8

DeFronzo RA, Tripathy D (2009) Skeletal muscle insulin resistance is the primary defect in type 2 diabetes https://doi.org/10.2337/dc09-S302

Donnelly C, Komlódi T, Cecatto C, Cardoso LHD, Compagnion AC, Matera A, Tavernari D, Campiche O, Paolicelli RC, Zanou N, Kayser B, Gnaiger E, Place N (2024) Functional hypoxia reduces

mitochondrial calcium uptake https://doi.org/10.1016/j.redox.2024.103037
Fontana L, Klein S, Holloszy JO (2010) Effects of long-term calorie restriction and endurance exercise on glucose tolerance, insulin action, and adipokine production https://doi.org/10.1007/s11357-009-9118-z
González A, Hall MN (2017) Nutrient sensing and TOR signaling in yeast and mammals https://doi.org/10.15252/embj.201696010
Heijboer AC, Donga E, Voshol PJ, Dang ZC, Havekes LM, Romijn JA, Corssmit EP (2005). Sixteen hours of fasting differentially affects hepatic and muscle insulin sensitivity in mice https://doi.org/10.1194/jlr.M400440-JLR200
Henver S Brunetta, Graham P Holloway (2022) A theoretical argument to support the biological benefits for insulin stimulating mitochondrial oxidative phosphorylation https://doi.org/10.1016/j.cophys.2022.100491
Herbers E, Kekäläinen NJ, Hangas A, Pohjoismäki JL, Goffart S (2019) Tissue specific differences in mitochondrial DNA maintenance and expression https://doi.org/10.1016/j.mito.2018.01.00
Holloszy JO (2011) Regulation of mitochondrial biogenesis and GLUT4 expression by exercise https://doi.org/10.1002/cphy.c100052
Holloszy JO (2013) "Deficiency" of mitochondria in muscle does not cause insulin resistance https://doi.org/10.2337/db12-1107
Jacovetti C, Abderrahmani A, Parnaud G, Jonas JC, Peyot ML, Cornu M, Laybutt R, Meugnier E, Rome S, Thorens B, Prentki M, Bosco D, Regazzi R (2012) MicroRNAs contribute to compensatory β cell expansion during pregnancy and obesity https://doi.org/10.1172/JCI64151
Jacovetti C, Bayazit MB, Regazzi R (2021) Emerging Classes of Small Non-Coding RNAs With Potential Implications in Diabetes and Associated Metabolic Disorders https://doi.org/10.3389/fendo.2021.670719
Jacovetti C, Donnelly C, Menoud V, Suleiman M, Cosentino C, Sobel J, Wu K, Bouzakri K, Marchetti P, Guay C, Kayser B, Regazzi R (2024) The mitochondrial tRNA-derived fragment, mt-tRF-Leu^{TAA}, couples mitochondrial metabolism to insulin secretion https://doi.org/10.1016/j.molmet.2024.101955
Jørgensen SW, Hjort L, Gillberg L, Justesen L, Madsbad S, Brøns C, Vaag AA (2021) Impact of prolonged fasting on insulin secretion, insulin action, and hepatic versus whole body insulin secretion disposition indices in healthy young males https://doi.org/10.1152/ajpendo.00433.2020
Kido K, Egawa T, Watanabe S, Kawanaka K, Treebak JT, Hayashi T (2022) Fasting potentiates insulin-mediated glucose uptake in rested and prior-contracted rat skeletal muscle https://doi.org/10.1152/ajpendo.00412.2021
Kim JA, Wei Y, Sowers JR (2008) Role of mitochondrial dysfunction in insulin resistance https://doi.org/10.1161/CIRCRESAHA.107.165472
Lampl T, Crum JA, Davis TA, Milligan C, Del Gaizo Moore V (2015) Isolation and functional analysis of mitochondria from cultured cells and mouse tissue https://doi.org/10.3791/52076
Laplante M, Sabatini DM (2012) mTOR signaling in growth control and disease https://doi.org/10.1016/j.cell.2012.03.017
Martins IP, de Oliveira JC, Pavanello A, Matiusso CCI, Previate C, Tófolo LP, Ribeiro TA, da Silva Franco CC, Miranda RA, Prates KV, Alves VS, Francisco FA, de Moraes AMP, de Freitas Mathias PC, Malta A (2018) Protein-restriction diet during the suckling phase programs rat metabolism against obesity and insulin resistance exacerbation induced by a high-fat diet in adulthood https://doi.org/10.1016/j.jnutbio.2018.03.017
Moore MC, Coate KC, Winnick JJ, An Z, Cherrington AD (2012) Regulation of hepatic glucose uptake and storage in vivo https://doi.org/10.3945/an.112.002089
Nesca V, Guay C, Jacovetti C, Menoud V, Peyot ML, Laybutt DR, Prentki M, Regazzi R (2013) Identification of particular groups of microRNAs that positively or negatively impact on beta cell function in obese models of type 2 diabetes https://doi.org/10.1007/s00125-013-2993-y

Nicholls DG (2016) The Pancreatic β-Cell: A Bioenergetic Perspective https://doi.org/10.1152/physrev.00009.2016

Nolan CJ, Prentki M (2019) Insulin resistance and insulin hypersecretion in the metabolic syndrome and type 2 diabetes: Time for a conceptual framework shift https://doi.org/10.1177/1479164119827611

Parker L, Trewin A, Levinger I, Shaw CS, Stepto NK (2017) The effect of exercise-intensity on skeletal muscle stress kinase and insulin protein signaling https://doi.org/10.1371/journal.pone.0171613

Petersen MC, Shulman GI (2018) Mechanisms of Insulin Action and Insulin Resistance https://doi.org/10.1152/physrev.00063.2017

Peyot ML, Pepin E, Lamontagne J, Latour MG, Zarrouki B, Lussier R, Pineda M, Jetton TL, Madiraju SR, Joly E, Prentki M (2010) Beta-cell failure in diet-induced obese mice stratified according to body weight gain: secretory dysfunction and altered islet lipid metabolism without steatosis or reduced beta-cell mass https://doi.org/10.2337/db09-1452

Prentki M, Nolan CJ (2006) Islet beta cell failure in type 2 diabetes https://doi.org/10.1172/JCI29103

Röder PV, Wu B, Liu Y, Han W (2016) Pancreatic regulation of glucose homeostasis https://doi.org/10.1038/emm.2016.6

Sivitz WI, Yorek MA (2010) Mitochondrial dysfunction in diabetes: from molecular mechanisms to functional significance and therapeutic opportunities https://doi.org/10.1089/ars.2009.2531

Suriano F, Vieira-Silva S, Falony G, Roumain M, Paquot A, Pelicaen R, Régnier M, Delzenne NM, Raes J, Muccioli GG, Van Hul M, Cani PD (2021) Novel insights into the genetically obese (ob/ob) and diabetic (db/db) mice: two sides of the same coin https://doi.org/10.1186/s40168-021-01097-8

Thorn SR, Rozance PJ, Brown LD, Hay WW Jr (2011) The intrauterine growth restriction phenotype: fetal adaptations and potential implications for later life insulin resistance and diabetes https://doi.org/10.1055/s-0031-1275516

Timper K, Paeger L, Sánchez-Lasheras C, Varela L, Jais A, Nolte H, Vogt MC, Hausen AC, Heilinger C, Evers N, Pospisilik JA, Penninger JM, Taylor EB, Horvath TL, Kloppenburg P, Brüning JC (2018) Mild Impairment of Mitochondrial OXPHOS Promotes Fatty Acid Utilization in POMC Neurons and Improves Glucose Homeostasis in Obesity https://doi.org/10.1016/j.celrep.2018.09.034

Titchenell PM, Lazar MA, Birnbaum MJ (2017) Unraveling the Regulation of Hepatic Metabolism by Insulin https://doi.org/10.1016/j.tem.2017.03.003

Trewin AJ, Parker L, Shaw CS, Hiam DS, Garnham A, Levinger I, McConell GK, Stepto NK (2018) Acute HIIE elicits similar changes in human skeletal muscle mitochondrial H2O2 release, respiration, and cell signaling as endurance exercise even with less work https://doi.org/10.1152/ajpregu.00096.2018

Vipin VA, Blesson CS, Yallampalli C (2022) Maternal low protein diet and fetal programming of lean type 2 diabetes https://doi.org/10.4239/wjd.v13.i3.185